

Undercomplete Blind Subspace Deconvolution via Linear Prediction

Zoltán Szabó, Barnabás Póczos, and András Lőrincz

Department of Information Systems, Eötvös Loránd University,
Pázmány P. sétány 1/C, Budapest H-1117, Hungary
WWW home page: <http://nipg.inf.elte.hu> (<http://nipg.info>)
sszoli@cs.elte.hu, pbarn@cs.elte.hu, andras.lorincz@elte.hu

Abstract. We present a novel solution technique for the blind subspace deconvolution (BSSD) problem, where temporal convolution of multidimensional hidden independent components is observed and the task is to uncover the hidden components using the observation only. We carry out this task for the undercomplete case (uBSSD): we reduce the original uBSSD task via linear prediction to independent subspace analysis (ISA), which we can solve. As it has been shown recently, applying temporal concatenation can also reduce uBSSD to ISA, but the associated ISA problem can easily become ‘high dimensional’ [6]. The new reduction method circumvents this dimensionality problem. We perform detailed studies on the efficiency of the proposed technique by means of numerical simulations. We have found several advantages: our method can achieve high quality estimations for smaller number of samples and it can cope with deeper temporal convolutions.

1 Introduction

There is a growing interest in independent component analysis (ICA) and blind source deconvolution (BSD) for signal processing and hidden component searches. ICA has been used for many purposes, including (i) feature extraction, (ii) denoising, (iii) processing of financial and neurobiological data, e.g. fMRI, EEG, and MEG. BSD has also shown potentials in several areas, for example (i) in remote sensing applications: passive radar/sonar processing, (ii) in image-deblurring and image restoration, (iii) in acoustics, including speech enhancement using microphone arrays, (iv) in multi-antenna wireless communications and in sensor networks, (v) in biomedical signal—EEG, ECG, MEG, fMRI—analysis, (vi) in optics, and (vii) in seismic exploration. For recent reviews in ICA and BSD themes see, e.g., [1, 2] and [3], respectively.

Traditionally, ICA is one-dimensional in the sense that all sources are assumed to be independent real valued stochastic variables. The traditional example of ICA is the so-called *cocktail-party problem*, where there are D sound sources and D microphones and the task is to separate the original sources from the observed mixed signals. Clearly, applications where not all, but only certain groups of the sources are independent may have high relevance in practice. In this

case, independent sources can be multidimensional. For example, there could be *independent groups of people* talking about independent topics at a conference, or *independent rock bands* may be playing at a party. This is the independent subspace analysis (ISA) extension of ICA [4]. Strenuous efforts have been made to develop ISA algorithms, where the theoretical problems concern mostly (i) the estimation of the entropy or of the mutual information, or (ii) joint block diagonalization. A recent list of possible ISA solution techniques can be found in [6].

Another extension of the original ICA task is the BSD problem [3], where the observation is a temporal mixture of the hidden components. Such a problem emerges, e.g., if the cocktail-party is held in an *echoic room*. A novel task, the blind subspace deconvolution (BSSD) [6] arises if we combine the ISA and the BSD assumptions. One can think of this task as the separation problem of the pieces played simultaneously by independent rock bands in an echoic stadium. One of the most stringent applications of BSSD could be the analysis of EEG or fMRI signals. The ICA assumptions could be highly problematic here, because some sources may depend on each other, so an ISA model seems better. Furthermore, the passing of information from one area to another and the related delayed and transformed activities may be modeled as echoes. Thus, one can argue that BSSD may fit this important problem domain better than ICA or even ISA. It has been shown in [6] that the undercomplete BSSD task (uBSSD)—where in terms of the cocktail-party problem there are more microphones than acoustic sources—can be reduced to ISA by means of temporal concatenation.¹ However, the reduction technique may lead to ‘high dimensions’ in the associated ISA problem. Here, an alternative reduction method solution is introduced for uBSSD and this solution avoids the increase of ISA dimensions. Namely, we show that one can apply the linear prediction method to reduce the uBSSD task to ISA such that the dimension of the associated ISA problem equals to the dimension of the original hidden sources. As an additional advantage, we shall see that this reduction principle is more efficient on problems with deeper temporal convolutions.

The paper is built as follows: Section 2 formulates the problem domain. Section 3 shows how to reduce the uBSSD task to an ISA problem. Section 4 contains the numerical illustrations. Section 5 contains a short summary.

2 The BSSD Model

We define the BSSD task in Section 2.1. Earlier BSSD reduction principles are reviewed in Section 2.2.

2.1 The BSSD Equations

Here, we define the BSSD task. Assume that we have M hidden, independent, multidimensional *components* (random variables). Suppose also that only their

¹ The complete, and in particular the overcomplete BSSD task is challenging and no general solution is known yet.

casual FIR filtered mixture is available for observation:

$$\mathbf{x}(t) = \sum_{l=0}^L \mathbf{H}_l \mathbf{s}(t-l), \quad (1)$$

where $\mathbf{s}(t) = [\mathbf{s}^1(t); \dots; \mathbf{s}^M(t)] \in \mathbb{R}^{Md}$ is a vector concatenated of components $\mathbf{s}^m(t) \in \mathbb{R}^d$. Here, for the sake of notational simplicity we used identical dimension for each component. For a given m , $\mathbf{s}^m(t)$ is i.i.d. (independent and identically distributed) in time t , there is at most one Gaussian in \mathbf{s}^m s, and $I(\mathbf{s}^1, \dots, \mathbf{s}^M) = 0$, where I stands for the mutual information of the arguments. The total dimension of the components is $D_s := Md$, the dimension of the observation \mathbf{x} is D_x . Matrices $\mathbf{H}_l \in \mathbb{R}^{D_x \times D_s}$ ($l = 0, \dots, L$) describe the convolutive mixing. Without any loss of generality it may be assumed that $E[\mathbf{s}] = \mathbf{0}$, where E denotes the expectation value. Then $E[\mathbf{x}] = \mathbf{0}$ holds, as well. The goal of the BSSD problem is to estimate the original source $\mathbf{s}(t)$ by using observations $\mathbf{x}(t)$ only. The case $L = 0$ corresponds to the ISA task, and if $d = 1$ also holds then the ICA task is recovered. In the BSD task $d = 1$ and L is a non-negative integer. $D_x > D_s$ is the *undercomplete*, $D_x = D_s$ is the *complete*, and $D_x < D_s$ is the *overcomplete* task. Here, we treat the undercomplete BSSD (uBSSD) problem.

For consecutive reductional steps we rewrite the BSSD model using operators. Let $\mathbf{H}[z] := \sum_{l=0}^L \mathbf{H}_l z^{-l} \in \mathbb{R}[z]^{D_x \times D_s}$ denote the $D_x \times D_s$ polynomial matrix corresponding to the convolutive mixing, in a one-to-one manner. Here, z is the time-shift operation, that is $(z^{-1}\mathbf{u})(t) := \mathbf{u}(t-1)$. Now, the BSSD equation (1) can be written as

$$\mathbf{x} = \mathbf{H}[z]\mathbf{s}. \quad (2)$$

In the uBSSD task it is assumed that $\mathbf{H}[z]$ has a polynomial matrix left inverse. In other words, there exists polynomial matrix $\mathbf{W}[z] \in \mathbb{R}[z]^{D_s \times D_x}$ such that $\mathbf{W}[z]\mathbf{H}[z]$ is the identity mapping. It can be shown [7] that for $D_x > D_s$ such a left inverse exists with probability 1, under mild conditions. The mild condition is as follows: Coefficients of polynomial matrix $\mathbf{H}[z]$, that is, the random matrix $[\mathbf{H}_0; \dots; \mathbf{H}_L]$ is drawn from a continuous distribution. For the ISA task it is supposed that mixing matrix $\mathbf{H}_0 \in \mathbb{R}^{D_x \times D_s}$ has full column rank, i.e., its rank is D_s .

2.2 Existing Decomposition Principles in the BSSD Problem Family

There are numerous reduction methods for the BSSD problem in the literature. For example, its special case, the undercomplete BSD task can be reduced (i) to ISA by temporal concatenation of the observations [8], or (ii) to ICA by means of either spatio-temporal decorrelation [9], or by linear prediction (autoregressive (AR) estimation) [10–12]. As it was shown in [6], the uBSSD task can also be reduced to ISA by temporal concatenation. In Section 3, we show another route and describe how linear prediction can help to transcribe the uBSSD task to ISA. According to the ISA Separation Theorem [6, 13], under certain conditions, the solution of the ISA task requires an ICA preprocessing step followed by a suitable

permutation of the ICA elements. This principle was conjectured in [4] on basis of numerical simulations. Only sufficient conditions are available in [6,13] for the ISA Separation Theorem. Possible reduction steps are shown in Fig. 1.

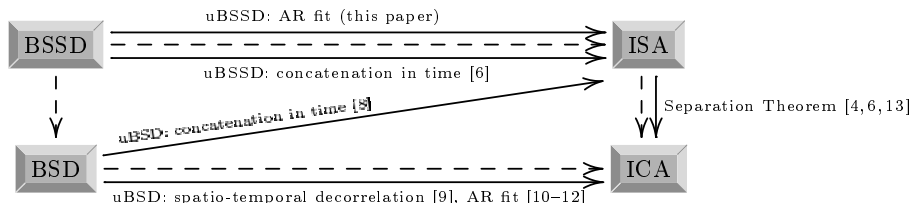


Fig. 1: Extensions of the ICA task. Prefix u denotes the undercomplete case. Dotted arrows point to special cases. Solid arrows indicate possible reductions. Respective reduction principles are noted at the arrows.

3 Reduction of uBSSD to ISA by Linear Prediction

Below, we reduce the uBSSD task to ISA by means of linear prediction. The procedure is similar to that of [12], where it was applied for undercomplete BSD (i.e., for $d = 1$).

Theorem. *In the uBSSD task, observation process $\mathbf{x}(t)$ is autoregressive and its innovation $\tilde{\mathbf{x}}(t) := \mathbf{x}(t) - E[\mathbf{x}(t)|\mathbf{x}(t-1), \mathbf{x}(t-2), \dots]$ is $\mathbf{H}_0\mathbf{s}(t)$, where $E[\cdot]$ denotes the conditional expectation value. Consequently, there is a polynomial matrix $\mathbf{W}_{\text{AR}}[z] \in \mathbb{R}[z]^{D_x \times D_x}$ such that $\mathbf{W}_{\text{AR}}[z]\mathbf{x} = \mathbf{H}_0\mathbf{s}$.*

Proof. We assumed that $\mathbf{H}[z]$ has left inverse, thus the hidden \mathbf{s} can be expressed from observation \mathbf{x} by causal FIR filtering, i.e., $\mathbf{s} = \mathbf{H}^{-1}[z]\mathbf{x}$, where $\mathbf{H}^{-1}[z] = \sum_{n=0}^N \mathbf{M}_n z^{-n} \in \mathbb{R}[z]^{D_s \times D_x}$ and N denotes the degree of the $\mathbf{H}^{-1}[z]$ polynomial. Thus, terms in observation \mathbf{x} that differ from $\mathbf{H}_0\mathbf{s}(t)$ in (1) belong to the linear hull of the finite history of \mathbf{x} : $\mathbf{x}(t) = \mathbf{H}_0\mathbf{s}(t) + \sum_{l=1}^L \mathbf{H}_l(\mathbf{H}^{-1}[z]\mathbf{x})(t-l) \in \mathbf{H}_0\mathbf{s}(t) + \langle \mathbf{x}(t-1), \mathbf{x}(t-2), \dots, \mathbf{x}(t-L+N) \rangle$. Because $\mathbf{s}(t)$ is independent of $\langle \mathbf{x}(t-1), \mathbf{x}(t-2), \dots, \mathbf{x}(t-L+N) \rangle$, we have that observation process $\mathbf{x}(t)$ is autoregressive with innovation $\mathbf{H}_0\mathbf{s}(t)$.

Thus, AR fit of $\mathbf{x}(t)$ can be used for the estimation of $\mathbf{H}_0\mathbf{s}(t)$. This innovation corresponds to the observation of an undercomplete ISA model², which can be reduced to a complete ISA using principal component analysis (PCA). Finally, the solution can be finished by any ISA procedure. The pseudocode of the above linear predictive approximation (LPA) method for the uBSSD task is given in Table 1.

² Assumptions made for $\mathbf{H}[z]$ in the uBSSD task implies that \mathbf{H}_0 is of full column rank and thus the resulting ISA task is well defined.

Table 1: Linear predictive approximation (LPA): Pseudocode

<p>Input of the algorithm Observation: $\{\mathbf{x}(t)\}_{t=1,\dots,T}$</p> <p>Optimization AR fit: for observation \mathbf{x} estimate $\hat{\mathbf{W}}_{\text{AR}}[z]$ Estimate innovation: $\tilde{\mathbf{x}} = \hat{\mathbf{W}}_{\text{AR}}[z]\mathbf{x}$ Reduce uISA to ISA and whiten: $\tilde{\mathbf{x}}' = \hat{\mathbf{W}}_{\text{PCA}}\tilde{\mathbf{x}}$ Apply ISA for $\tilde{\mathbf{x}}'$: separation matrix is $\hat{\mathbf{W}}_{\text{ISA}}$</p> <p>Estimation $\hat{\mathbf{W}}_{\text{uBSSD}}[z] = \hat{\mathbf{W}}_{\text{ISA}}\hat{\mathbf{W}}_{\text{PCA}}\hat{\mathbf{W}}_{\text{AR}}[z]$ $\hat{\mathbf{s}} = \hat{\mathbf{W}}_{\text{uBSSD}}[z]\mathbf{x}$</p>

The reduction procedure implies that hidden components \mathbf{s}^m can be recovered only up to the ambiguities of the ISA task. The ISA ambiguities are simple [14]: hidden multidimensional components can be determined up to permutation and up to invertible transformation within the subspaces. Furthermore, in the ISA model it can be assumed without any loss of generality, that both the hidden source (\mathbf{s}) and the observation are white; their expectation values are zeroes and the covariance matrices are identities. Now, the \mathbf{s}^m components are determined up to permutation and orthogonal transformation.

4 Illustrations

We show the results of our studies concerning the efficiency of the algorithm of Table 1. We compare the LPA procedure with the uBSSD method described in [6]. There temporal concatenation was applied to transform the uBSSD task to a ‘high-dimensional’ ISA task. We shall refer to that method as the method of temporal concatenation, or TCC for short. Test problems are introduced in Section 4.1. The performance index that we use to measure the quality of the solutions is detailed in Section 4.2. Numerical results are presented in Section 4.3.

4.1 Databases

We define four databases (\mathbf{s}) to study our LPA algorithm. These are the databases used in [6], too. In the *3D-geom* test hidden components \mathbf{s}^m are random variables uniformly distributed on 3-dimensional geometric forms ($d = 3$). We have 6 components ($M = 6$). The dimension of the hidden source \mathbf{s} is $D_s = 18$. See Fig. 2(a). The *celebrities* test has 10 of 2-dimensional source components generated from cartoons of celebrities ($d = 2$).³ The 2-dimensional images of celebrities are considered as the density functions of \mathbf{s}^m : sources are generated according to the pixel intensities. See Fig. 2(b). In the *letters* data set, hidden sources \mathbf{s}^m are uniformly distributed on 2-dimensional images ($d = 2$) of

³ <http://www.smileyworld.com>

letters A and B. The number of components and the dimension of the sources are minimal ($M = 2$, $D_s = 4$). See Fig. 2(c). Our *Beatles* test is a non-i.i.d. example. Here, hidden sources are stereo Beatles songs.⁴ 8 kHz sampled portions of two songs (A *Hard Day's Night*, *Can't Buy Me Love*) made the hidden \mathbf{s}^m s ($d = 2$, $M = 2$, $D_s = 4$).

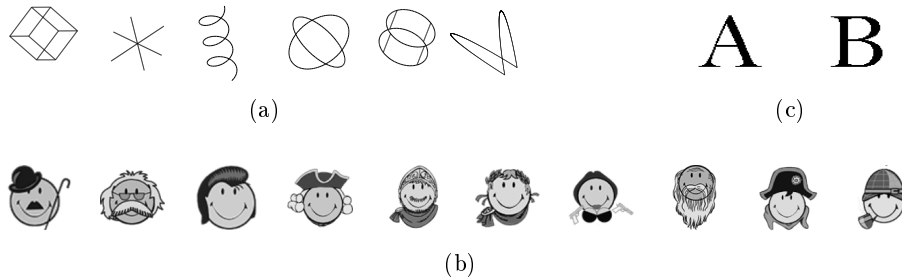


Fig. 2: Illustration of the *3D-geom*, *celebrities* and *letters* databases. (a): Database *3D-geom* contains 6 of 3-dimensional components ($M = 6$, $d = 3$). Hidden sources are uniformly distributed variables on 3-dimensional geometric objects. (b): Database *celebrities* contains 10 of 2-dimensional components ($M = 10$, $d = 2$). Density functions of the hidden sources (\mathbf{s}^m) are proportional to the pixel intensities of the 2-dimensional images. (c): *Letters* database is minimal. Hidden sources \mathbf{s}^m are uniformly distributed on images of letters A and B ($M = 2$, $d = 2$).

4.2 The Amari-index

According to Section 3, in the ideal case, the product of matrix $\hat{\mathbf{W}}_{\text{ISA}} \hat{\mathbf{W}}_{\text{PCA}}$ (the result of PCA and ISA) and matrix \mathbf{H}_0 , that is matrix $\mathbf{G} := \hat{\mathbf{W}}_{\text{ISA}} \hat{\mathbf{W}}_{\text{PCA}} \mathbf{H}_0 \in \mathbb{R}^{D_s \times D_s}$ is a block-permutation matrix made of $d \times d$ blocks. To measure this block-permutation property, we used the normalized version [13] of the Amari-error [15] adapted to the ISA task [5]. Namely, let matrix $\mathbf{G} \in \mathbb{R}^{D_s \times D_s}$ be decomposed into $d \times d$ blocks: $\mathbf{G} = [\mathbf{G}^{i,j}]_{i,j=1,\dots,M}$. Let $g^{i,j}$ denote the sum of the absolute values of the elements of matrix $\mathbf{G}^{i,j} \in \mathbb{R}^{d \times d}$. Now, the normalized Amari-error, the Amari-index ($r(\cdot) = r_{d,D_s}(\cdot)$) is defined as:

$$r(\mathbf{G}) := \frac{1}{2M(M-1)} \left[\sum_{i=1}^M \left(\frac{\sum_{j=1}^M g^{i,j}}{\max_j g^{i,j}} - 1 \right) + \sum_{j=1}^M \left(\frac{\sum_{i=1}^M g^{i,j}}{\max_i g^{i,j}} - 1 \right) \right].$$

For matrix \mathbf{G} we have that $0 \leq r(\mathbf{G}) \leq 1$. $r(\mathbf{G}) = 0$ if, and only if \mathbf{G} is a block-permutation matrix with $d \times d$ sized blocks. Thus, $r(\mathbf{G}) = 0$ for a perfect \mathbf{G} , whereas in the worst case $r(\mathbf{G}) = 1$. Given that index r takes values in $[0, 1]$

⁴ <http://rock.mididb.com/beatles/>

independently from d and D_s , we can use this measure to compare the TCC and LPA techniques.

4.3 Simulations

Results on databases *3D-geom*, *celebrities*, *letters* and *Beatles* are provided here. The experimental studies concern two questions:

1. The TCC and the LPA methods are compared on uBSSD tasks.
2. The performance as a function of convolution length is studied for the LPA technique.

Our test databases correspond to those of [6] and here, we study the $D_x = 2D_s$ case, like in the cited reference. Both the TCC and the LPA method reduce the uBSSD task to ISA problems and we use the Amari-index (Section 4.2) to measure and compare their performances. For all values of the parameters (sample number: T , convolution length: $L + 1$), we have averaged the performances upon 50 random initializations of \mathbf{s} and $\mathbf{H}[z]$. The coordinates of matrices \mathbf{H}_l were chosen independently from standard normal distribution. We used the Schwarz’s Bayesian Criterion [16] to determine the optimal order of the AR process. The criterion was constrained: the order Q of the estimated AR process (see Table 1) was limited from above, the upper limit was set to twice the length of the convolution, i.e., $Q \leq 2(L + 1)$. The AR process was then estimated by the method detailed in [16] and [17]. Both in the case of TCC and in the case of LPA, ISA was accomplished by joint f-decorrelation (JFD) as detailed in [18].

We studied the dependence of the precision versus the sample number on databases *3D-geom* and *celebrities*. The dimension and the number of the components were $d = 3$ and $M = 6$ for the *3D-geom* database and $d = 2$ and $M = 10$ for the *celebrities* database, respectively. In both cases the sample number T varied between 1,000 and 100,000. The length of the convolution ($L + 1$) changed between 2 and 6. Comparisons with the TCC method are shown in Figs. 3(a)-(d). LPA estimation errors are given in Table 2. Figures 4(a)-(d) and (i)-(l) illustrate the estimations of the LPA technique on the *3D-geom* and on the *celebrities* databases, respectively.

	$L = 1$	$L = 2$	$L = 3$	$L = 4$	$L = 5$
3D-geom	0.20% (± 0.01)	0.20% (± 0.02)	0.19% (± 0.02)	0.20% (± 0.02)	0.20% (± 0.01)
celebrities	0.33% (± 0.02)	0.33% (± 0.02)	0.34% (± 0.02)	0.34% (± 0.02)	0.34% (± 0.02)

Table 2: The Amari-index of the LPA method for database *3D-geom* and *celebrities*, for different convolution lengths: average \pm deviation. Number of samples: $T = 100,000$. For other sample numbers between $1,000 \leq T < 100,000$, see Figs. 3(a) and (c).

Figures 3(a) and (c) demonstrate that the LPA algorithm is able to uncover the hidden components with high precisions. The Amari-index r decreases

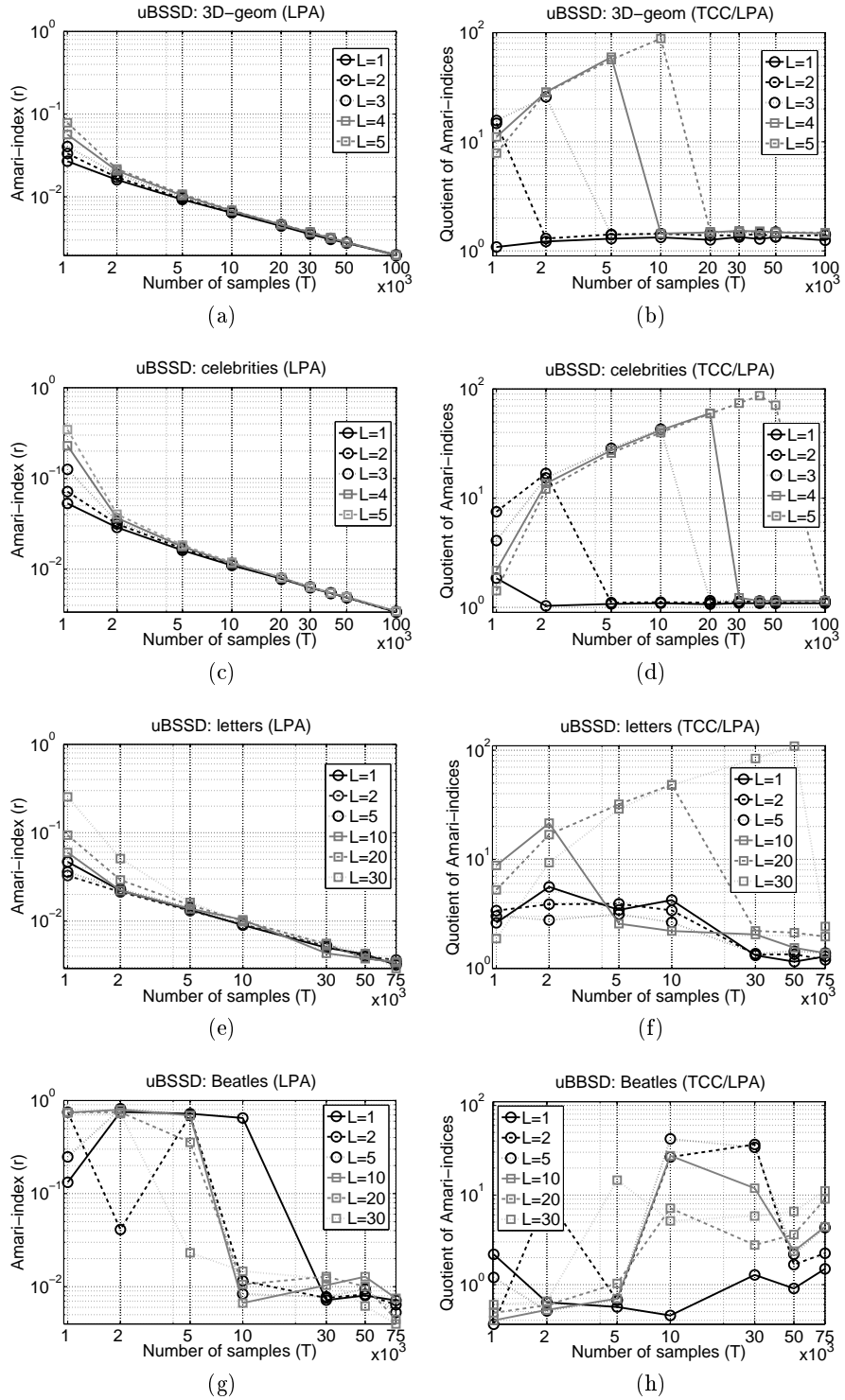


Fig. 3: Estimation error of the LPA method and comparisons with the TCC method for the *3D-geom*, the *celebrities*, the *letters* and the *Beatles* databases. Scales are 'log log' plots. Data correspond to different convolution lengths ($L + 1$). (a), (c), (e) and (g): Amari-index as a function of sample number for the *3D-geom*, *celebrities*, *letters* and *Beatles* databases. (b), (d), (f) and (h): Quotients of the Amari-indices of the TCC and the LPA methods: for quotient value $q > 1$, the LPA method is q times more precise than the TCC method.

according to power law $r(T) \propto T^{-c}$ ($c > 0$) for sample numbers $T > 2000$. The power law is manifested by straight lines on loglog scales. According to Figs. 3(b) and (d), the LPA method is superior to the TCC method (i) for all sample numbers $1,000 \leq T \leq 100,000$, moreover (ii) LPA can provide reasonable estimates for much smaller sample numbers. This behavior is manifested by the initial steady increase of the quotients of the Amari indices of the TCC and LPA methods as a function of sample number followed by a sudden drop when the sample number enables reasonable TCC estimations, too. The LPA method resulted in 1.1 – 88-times increase of precision for the *3D-geom* database and a similar 1.0 – 87-times increase for the *celebrities* database. According to Table 2, the Amari-index for sample number $T = 100,000$ is 0.19 – 0.20% (0.33 – 0.34%) with small 0.01 – 0.02 (0.02) standard deviations for the *3D-geom* (*celebrities*) database. Figures 4(e)-(h) and (m)-(q) demonstrate that the LPA method may provide acceptable estimations for reasonably small ($T = 20,000$) sample numbers up to convolution depth $L = 20$.

In our test on ‘*letters*’ and ‘*Beatles*’ the number of components and their dimensions were minimal ($d = 2, M = 2$). According to Figs. 3(e) and (g), the LPA method found the hidden components. For the *letters* dataset, the ‘power law’ decline of the Amari-index, that was apparent in the *3D-geom* and the *celebrities* databases, appears too. For this dataset, Fig. 3(f) shows that the LPA method is more precise than the TCC method for all sample numbers. The quotient is between 1.2 – 110, and the form of the curve is similar to those of the *3D-geom* and *celebrities* databases. According to Table 3, for sample number $T = 75,000$ the Amari-index stays below 1% on average (0.3 – 0.36%) and has 0.11 – 0.15 standard deviation. Visual inspection of Fig. 3(g) shows that the LPA method found the hidden components for sample number $T \geq 30,000$ on the *Beatles* database. We found that the TCC method gave reliable solutions for sample number $T = 50,000$ or so. In addition, according to Fig. 3(h) the LPA method is more precise for $T \geq 30,000$ than the TCC technique. The increase in precision becomes more pronounced for larger convolution parameter L . Namely, for sample number 75,000 and for $L = 1, 2, 5, 10, 20, 30$ the ratios of precision are 1.50, 2.24, 4.33, 4.42, 9.03, 11.13, respectively on the average. According to Table 3, for sample number $T = 75,000$ the Amari-index stays below 1% on average (0.4 – 0.71%) and has 0.02 – 0.08 standard deviation for the *Beatles* test.

$L = 1$	$L = 2$	$L = 5$	$L = 10$	$L = 20$	$L = 30$
0.32%(± 0.11)	0.36%(± 0.14)	0.34%(± 0.13)	0.34%(± 0.15)	0.34%(± 0.11)	0.30%(± 0.14)
0.71%(± 0.06)	0.64%(± 0.07)	0.53%(± 0.02)	0.75%(± 0.07)	0.45%(± 0.08)	0.40%(± 0.06)

Table 3: The Amari-index of the LPA method for database *letters* and *Beatles* for different convolution lengths: average \pm deviation. Number of samples: $T = 75,000$. First row: *letters*, second row: *Beatles* test. For other sample numbers between $1,000 \leq T < 75,000$, see Figs. 3(e) and (g).

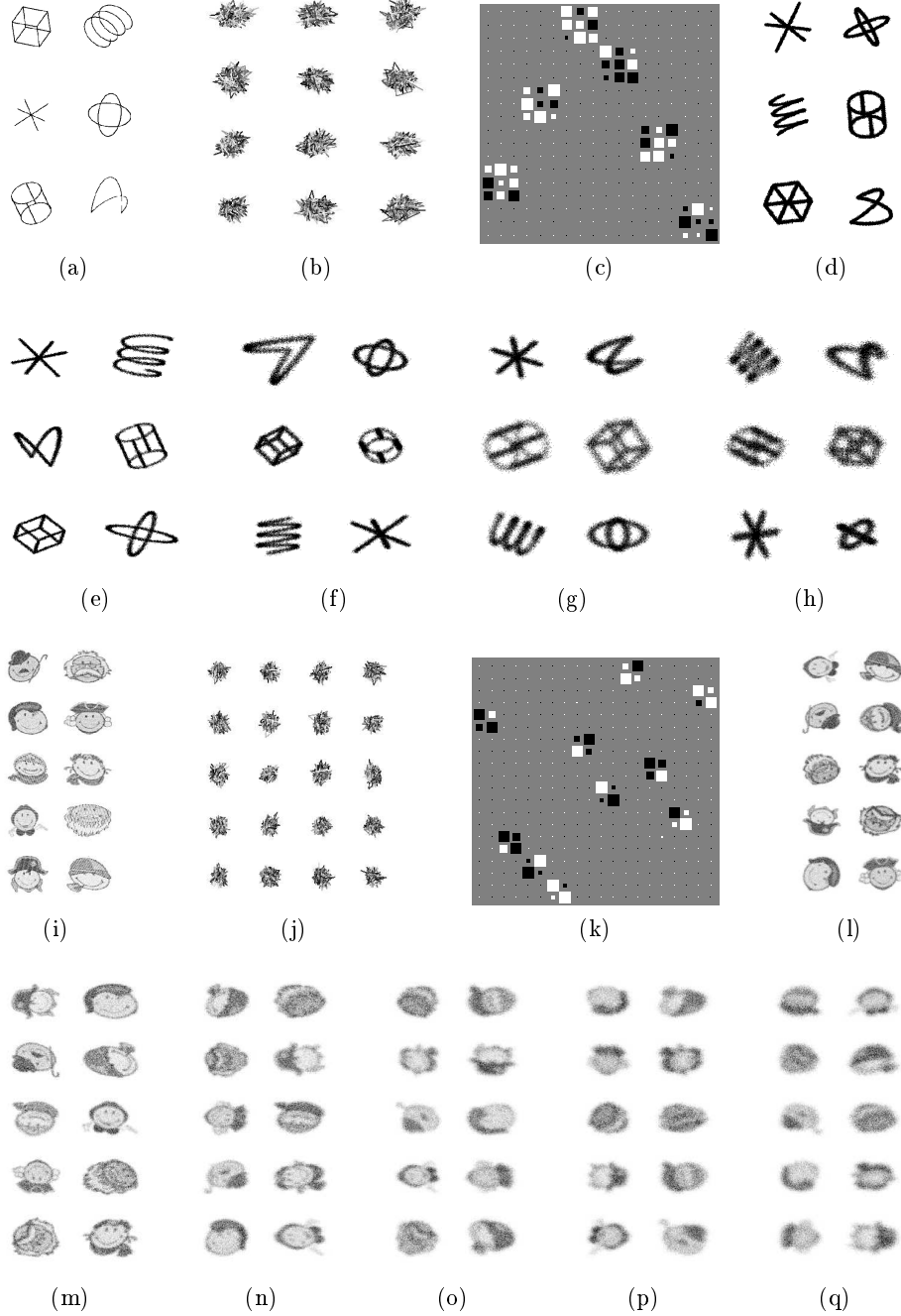


Fig. 4: Illustration of the LPA method on the uBSSD task for the *3D-geom* and *celebrities* databases. (a)-(d), (i)-(l): sample number $T = 100,000$, convolution length $L + 1 = 6$. (a) and (i): hidden components $\mathbf{s}^m(t)$. (b) and (j): observed convolved signals $\mathbf{x}(t)$, only 1000 time steps are shown. (c) and (k): Hinton-diagram of \mathbf{G} , ideally block-permutation matrix with 2×2 (3×3) blocks. (d) and (l): estimated components $(\hat{\mathbf{s}}^m)$, Amari-indices: 0.2% and 0.34%, respectively. (e)-(h) and (m)-(q): sample number $T = 20,000$, dependence of estimated components $(\hat{\mathbf{s}}^m)$ on the convolution parameter L . L is 1, 5, 10, 20, and 1, 5, 10, 15, 20 respectively.

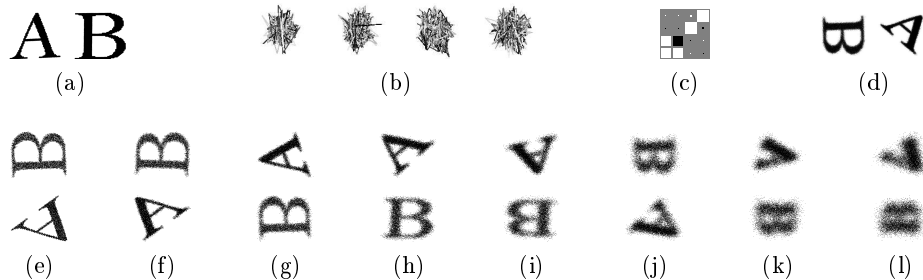


Fig. 5: Illustration of the LPA method on the uBSSD task for the *letters* database. (a)-(d): sample number $T = 75,000$, convolution length $L + 1 = 31$, Amari-index 0.3%. (a): hidden components $\mathbf{s}^m(t)$. (b): observed convolved signals $\mathbf{x}(t)$, only 1000 time steps are shown. (c): Hinton-diagram of \mathbf{G} , ideally block-permutation matrix with 2×2 blocks. (d): estimated components ($\hat{\mathbf{s}}^m$). (e)-(l): dependence of estimated components ($\hat{\mathbf{s}}^m$) on the convolution parameter L . L is 1, 5, 10, 20, 50, 100, 200, 230, respectively. Sample number is $T = 15,000$.

Both for database *letters* and database *Beatles*, the estimations are acceptable up to about $L = 230$ convolution depths for sample number $T = 15,000$. We illustrate this in Figs. 5(e)-(l) for the *letters* database with average Amari-index estimations.

5 Summary

We showed a novel solution method for the undercomplete case of the blind subspace deconvolution (uBSSD) task. We used a stepwise decomposition principle and reduced the problem with linear prediction to independent subspace analysis (ISA) task. We illustrated the method on different tests. Our method supersedes the temporal concatenation based uBSSD method, because (i) it gives rise to a smaller dimensional ISA task, (ii) it produces similar estimation errors at considerably smaller sample numbers, and (iii) it can treat deeper temporal convolutions.

References

1. Hyvärinen, A., Karhunen, J., Oja, E.: Independent Component Analysis. John Wiley & Sons (2001)
2. Cichocki, A., Amari, S.: Adaptive blind signal and image processing. John Wiley & Sons (2002)
3. Pedersen, M.S., Larsen, J., Kjems, U., Parra, L.C.: A survey of convolutive blind source separation methods. In: Springer Handbook of Speech (to appear). Springer Press (2007) (<http://www2.imm.dtu.dk/pubdb/p.php?4924>).

4. Cardoso, J.: Multidimensional independent component analysis. In: International Conference on Acoustics, Speech, and Signal Processing (ICASSP '98). Volume 4. (1998) 1941–1944
5. Theis, F.J.: Blind signal separation into groups of dependent signals using joint block diagonalization. In: International Society for Computer Aided Surgery (IS-CAS '05). (2005) 5878–5881
6. Szabó, Z., Póczos, B., Lőrincz, A.: Undercomplete blind subspace deconvolution. *Journal of Machine Learning Research* (2007) (accepted; preliminary version is available at <http://arxiv.org/abs/math.ST/0701210>).
7. Rajagopal, R., Potter, L.C.: Multivariate MIMO FIR inverses. *IEEE Transactions on Image Processing* **12** (2003) 458 – 465
8. Févotte, C., Doncarli, C.: A unified presentation of blind source separation for convolutive mixtures using block-diagonalization. In: Independent Component Analysis and Blind Signal Separation (ICA '03). (2003) 349–354
9. Choi, S., Cichocki, A.: Blind signal deconvolution by spatio-temporal decorrelation and demixing. *Neural Networks for Signal Processing* **7** (1997) 426–435
10. Icart, S., Gautier, R.: Blind separation of convolutive mixtures using second and fourth order moments. In: International Conference on Acoustics, Speech, and Signal Processing (ICASSP '96). Volume 5. (1996) 3018–3021
11. Delfosse, N., Loubaton, P.: Adaptive blind separation of convolutive mixtures. In: International Conference on Acoustics, Speech, and Signal Processing (ICASSP '96). (1996) 2940–2943
12. Gorokhov, A., Loubaton, P.: Blind identification of MIMO-FIR systems: A generalized linear prediction approach. *Signal Processing* **73** (1999) 105–124
13. Szabó, Z., Póczos, B., Lőrincz, A.: Cross-entropy optimization for independent process analysis. In: Independent Component Analysis and Blind Signal Separation (ICA '06). Volume 3889 of LNCS., Springer (2006) 909–916
14. Theis, F.J.: Uniqueness of complex and multidimensional independent component analysis. *Signal Processing* **84** (2004) 951–956
15. Amari, S., Cichocki, A., Yang, H.H.: A new learning algorithm for blind signal separation. *Advances in Neural Information Processing Systems* **8** (1996) 757–763
16. Neumaier, A., Schneider, T.: Estimation of parameters and eigenmodes of multivariate autoregressive models. *ACM Transactions on Mathematical Software* **27** (2001) 27–57
17. Schneider, T., Neumaier, A.: Algorithm 808: ARfit - a matlab package for the estimation of parameters and eigenmodes of multivariate autoregressive models. *ACM Transactions on Mathematical Software* **27** (2001) 58–65
18. Szabó, Z., Lőrincz, A.: Real and complex independent subspace analysis by generalized variance. In: ICA Research Network International Workshop (ICARN '06). (2006) 85–88 (<http://arxiv.org/abs/math.ST/0610438>).